Chapter 8
Fuzzy Fibers: Uncertainty in dMRI Tractography

Thomas Schultz, Anna Vilanova, Ralph Brecheisen and Gordon Kindlmann

Abstract Fiber tracking based on diffusion weighted Magnetic Resonance Imaging (dMRI) allows for noninvasive reconstruction of fiber bundles in the human brain. In this chapter, we discuss sources of error and uncertainty in this technique, and review strategies that afford a more reliable interpretation of the results. This includes methods for computing and rendering probabilistic tractograms, which estimate precision in the face of measurement noise and artifacts. However, we also address aspects that have received less attention so far, such as model selection, partial voluming, and the impact of parameters, both in preprocessing and in fiber tracking itself. We conclude by giving impulses for future research.

8.1 Introduction

Diffusion weighted MRI (dMRI) is a modern variant of Magnetic Resonance Imaging that allows for noninvasive, spatially resolved measurement of apparent self-diffusion

T. Schultz (✉)
University of Bonn, Bonn, Germany
e-mail: schultz@cs.uni-bonn.de

T. Schultz
MPI for Intelligent Systems,University of Bonn, Tübingen, Germany

A. Vilanova
TU Delft, Delft, Netherlands
e-mail: a.vilanova@tudelft.nl

A. Vilanova · R. Brecheisen
TU Eindhoven, Eindhoven, Netherlands
e-mail: r.brecheisen@tue.nl

G. Kindlmann
University of Chicago, Chicago, USA
e-mail: glk@uchicago.edu

C.D. Hansen et al. (eds.), *Scientific Visualization*, Mathematics and Visualization,
DOI 10.1007/978-1-4471-6497-5_8

coefficients. Since fibrous tissues such as nerve fiber bundles in the human brain constrain water molecules such that they diffuse more freely along fibers than orthogonal to them, the apparent diffusivity depends on the direction of measurement, and allows us to infer the main fiber direction.

Based on such data, tractography algorithms reconstruct the trajectories of major nerve fiber bundles. The most classic variant is streamline tractography, in which tracking starts at some seed point and proceeds in small steps along the inferred direction. In its simplest form, this results in one space curve per seed point. It has been observed that many of the resulting streamlines agree with known anatomy [11]. Tractography is also supported by validation studies that have used software simulations, physical and biological phantoms [25].

Tractography is currently the only technique for noninvasive reconstruction of fiber bundles in the human brain. This has created much interest among neuroscientists, who are looking for evidence of how connectivity between brain regions varies between different groups of subjects [60], as well as neurosurgeons, who would like to know the exact spatial extent of specific fiber bundles in individual patients.

However, drawing reliable inference from dMRI is challenging. Even though a randomized controlled study has shown that using dMRI in cerebral glioma surgery reduces postoperative motor deficits and increases survival times [68], neurosurgeons have observed that some methods for tractography underestimate the true size of bundles [37] and they are still unsatisfied with the degree of reproducibility that is achieved with current software packages [9].

In order to establish tractography as a reliable and widely accepted technique, it is essential to gain a full understanding of its inherent sources of error and uncertainty. It is the goal of this chapter to give an introduction to these problems, to present existing approaches that have tried to mitigate or model them, and to outline some areas where more work is still needed.

8.2 Noise and Artifacts

8.2.1 Strategies for Probabilistic Tractography

It is the goal of probabilistic tractography to estimate the variability in fiber bundle reconstructions that is due to measurement noise. This is often referred to as precision of the reconstructed bundle trajectory [33]. Due to additional types of error in data acquisition and modeling, which will be covered later in this chapter, it is not the same as accuracy (i.e., likelihood of a true anatomical connection) [35]. Current approaches do not account for factors such as repositioning of the head or variations in scanner hardware over time, which further affect repeatability in practice.

Rather than only inferring the most likely fiber direction, probabilistic approaches derive a probability distribution of fiber directions from the data. The first generation of probabilistic tractography methods has done so by fitting the diffusion tensor model

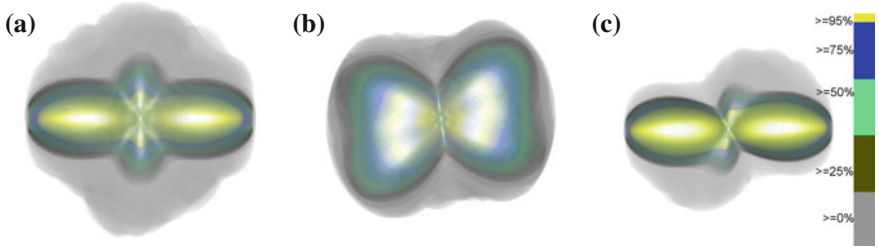

Fig. 8.1 Volume rendering ensembles of orientation distribution functions highlights regions that are included in most ensemble members. Subfigures **a–c** compare the uncertainty resulting from different fiber configurations and measurement setups. Images provided by the authors of [28]. **a** $b = 4{,}000$, SNR $= 5$, **b** $b = 7{,}000$, SNR $= 10$, **c** $b = 7{,}000$, SNR $= 10$

to the data, and using the result to parameterize a probability distribution in a heuristic manner. This often assumes that the fiber distribution is related to a sharpened version of the diffusivity profile [38], sometimes regularized by a deliberate bias towards the direction of the previous tracking step [4, 19]. Programmable graphics hardware accelerates the sampling of such models, and enables immediate visualization of the results [40]. Parker et al. [45] present two different fiber distribution models that are parameterized by measures of diffusion anisotropy. Subsequent work allows for multimodal distributions that capture fiber crossings, and uses the observed variation of principal eigenvectors in synthetic data to calibrate model parameters [44].

In contrast to these techniques, which use the model parameters from a single fit, a second generation of probabilistic tractography methods estimates the posterior distribution of fiber model parameters, based on the full information from the measurements, which includes fitting residuals. Behrens et al. [3] do so in an objective Bayesian framework, which aims at making as few assumptions as possible, by choosing noninformative priors. They have later extended the "ball-and-stick" model that underlies their framework to allow for multiple fiber compartments [2].

Bootstrapping estimates the distribution of anisotropy measures [43] or fiber directions [31, 55] by repeated model fitting, after resampling data from a limited number of repeated scans. This has been used as the foundation of another line of probabilistic tractography approaches [35, 39]. As an alternative to estimating the amount of noise from repeated measurements, wild bootstrapping takes its noise estimates from the residuals that remain when fitting a model to a single set of measurements [67]. This has been proposed as an alternative to repetition-based bootstrapping for cases where only a single acquisition is available [32]. Residual bootstrapping [12] builds on the same basic idea, but allows for resampling residuals between gradient directions, by modeling the heteroscedasticity in them. It has not only been combined with the diffusion tensor model, but also with constrained deconvolution, which allows for multiple fiber tractography [27].

To visualize the distributions estimated by bootstrapping, Jiao et al. [28] volume render ensembles of orientation distribution functions (ODFs). As shown in Fig. 8.1, this highlights regions included in most ensemble members, representing the most

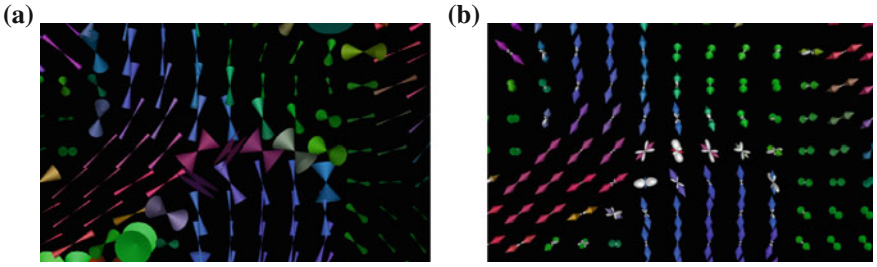

Fig. 8.2 Uncertainty in fiber directions has been visualized using cones of uncertainty, which include 95 % of all estimated directions (**a**) [31] The characteristics of the distribution are shown in greater detail by HiFiVE glyphs, which decompose it into a main direction, shown as *colored double cones*, and a residual PDF, shown as a *gray surface* (**b**) [55]

certain part of the ODF. For tractography, the main features of interest are the inferred fiber directions. The uncertainty in these directions has traditionally been visualized using cones that represent 95 % confidence intervals around a main direction [31]. Figure 8.2 compares this approach to the alternative, more recent HiFiVE glyph, which provides a more detailed impression of the distribution [55].

8.2.2 Rendering Probabilistic Tractograms

After estimating the reproducibility of white matter fiber tracts by one of the above-described methods, we can represent the results in one of two ways: voxel-centric or tract-centric. The voxel-centric representation assigns scores to individual voxels, where each voxel stores the percentage of tracts passing through it. They represent the reproducibility with which a connection from one voxel position to the seeding region is inferred from the data. The resulting 3D volume data sets are sometimes called probability or confidence maps, and are often visualized by volume rendering techniques, as in Fig. 8.3b, and 2D color maps [40].

Tract-centric techniques include the ConTrack algorithm [59], which assigns a score to each generated tract. It reflects confidence in the pathway as a whole, based on its agreement with the data and assumptions on fiber length and smoothness. Ehricke et al. [15] define a confidence score that varies along the fiber, and color code it on the streamline. Jones et al. [30, 32] use hyperstreamlines to visualize the variability of fiber tracts obtained using bootstrap or wild-bootstrap methods. They also demonstrate that using standard streamlines to render all fiber variations equally fails to give an impression of which fibers are stable and which are outliers.

Brecheisen et al. [6] propose illustrative confidence intervals where intervals are based on distances or pathway scores. Illustrative techniques, i.e., silhouette and outlines, are used to visualize these intervals. Interaction and Focus+Context widgets are used to extend the simplified illustrative renderings with more detailed information.

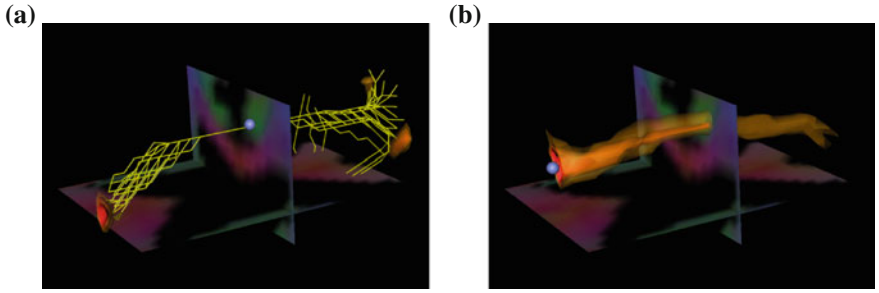

Fig. 8.3 Equally rendering all fiber variations from a seed (*blue ball*) as standard streamlines (**a**) makes it difficult to see which of them are most stable, and which are isolated outliers. Volumetric representations (**b**) are a popular alternative. Images from [53]. **a** Tract-centric visualization, showing all streamlines traced from a common seed. **b** Nested isosurfaces indicate different levels of confidence

Schultz et al. [57] cluster the voxels in which probabilistic tractography terminates, based on the seed points from which they are reached. They then derive a per-voxel score that indicates how frequently the voxel was involved in a connection between two given clusters. Fuzzy fiber bundle geometry is defined by isosurfaces of this score, with different isovalues representing different levels of precision.

8.3 Other Factors

8.3.1 Impact of Parameters

One source of uncertainty in dMRI tractography that has not received much attention is parameter sensitivity. Most tractography algorithms depend on user-defined parameters, which results in a poor reproducibility of the output results. Some reproducibility studies for concrete applications have been reported [13, 65]. However, there does not exist an automatic solution that resolves the problem in a general manner. The stability of the parameter setting is relevant information for both neuroscientists and neurosurgeons who are trying to assess whether their fiber tracking results are stable. Visualization can play an important role to help this assessment.

Brecheisen et al. [7] build a parameter space by sampling combinations of stopping criteria for DTI streamline tractography. Stopping criteria primarily affect fiber length. The investigation of parameter sensitivity is based on generating a streamline set that covers the whole parameter space of stopping criteria. Afterwards, selective culling is performed to display specific streamline collections from the parameter space. This is done by selecting parameter combinations using 2D widgets such as the feature histogram displayed in Fig. 8.4. An example feature is average fiber density per voxel. These views help the user to identify stable parameter settings, thereby improving the ability to compare groups of subjects based on quantitative tract features.

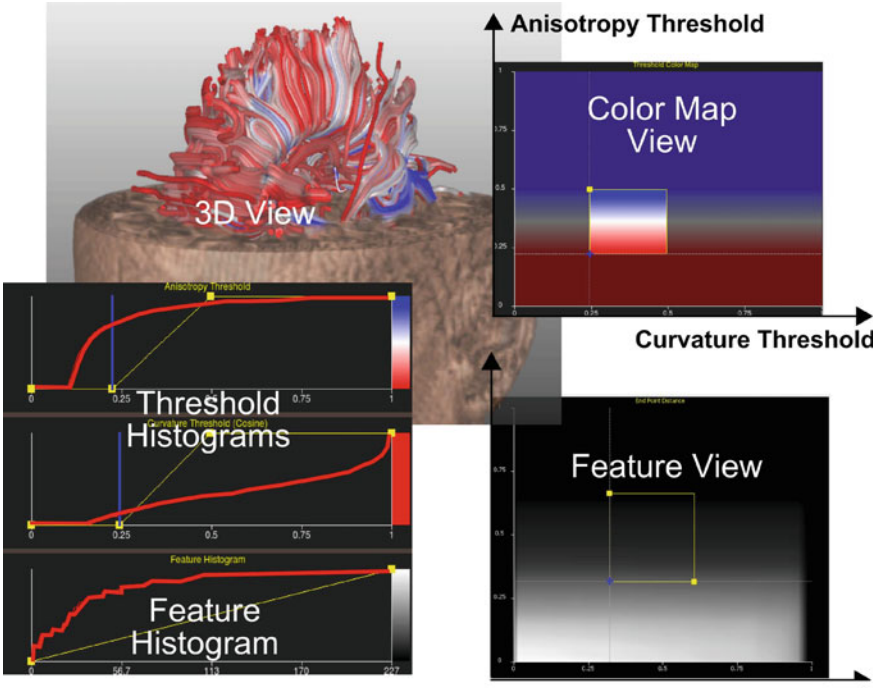

Fig. 8.4 Main viewports of Brecheisen et al. [7] exploration tool. *Top-left* 3D visualization of fiber tract together with anatomical context and axial fractional anisotropy slice. *Top-right* Color map view used for selecting individual threshold combinations and definition of color detail regions. *Bottom-right* Feature map view showing changes in quantitative tract features as a function of threshold combination at discrete sample points of the parameter space. *Bottom-left* Cumulative histograms of both threshold and feature values. © IEEE Reprinted, with permission, from IEEE Transactions on Visualization and Computer Graphics 15(6)

Jiao et al. [29] introduce a toolkit based on three streamline distances that are used to measure differences between fiber bundles. The user can vary parameters that affect the results of the fiber tractography and measure the resulting differences based on these distances. This allows them to quantify the variation and reproducibility of the fiber bundles due to different sources of uncertainty and variation in the tractography input parameters.

Although these methods provide a first step to study uncertainty due to parameter settings, it remains a time consuming exploratory task for the user. This is especially true if parameters are correlated, and their interrelation needs to be investigated.

8.3.2 Model Uncertainty and Selection

Methods for tractography that seek to recover more than a single fiber direction in a given area have to make a judgement about how many fiber directions can be meaningfully recovered from the dMRI data. The combination of measurement noise, partial voluming, and the practical constraints on how many diffusion weighted images may be acquired create uncertainty in the number of fibers present. Qualitatively different than the angular uncertainty in a single fiber direction, the traditional focus of probabilistic tractography, this uncertainty can be a viewed as a kind of *model selection uncertainty*, which is described further in Sect. 8.4.1.

Uncertainty in fiber number has been handled by different tests that either statistically sample or deterministically choose a level of model complexity (with an associated fiber number) from a nested set of models. Behrens et al. [2] use Automatic Relevance Determination (ARD) to probabilistically decide the number of "sticks" (fibers) in their ball-and-multiple-stick model. Within their probabilistic tractography, this achieves Bayesian Model Averaging [22] of the fiber orientation. For deterministic tractography, Qazi et al. [50] use a threshold on the (single, second-order) tensor planarity index c_p [66] to determine whether to fit to the diffusion weightes images a constrained two-tensor model [46] that permits tracing two crossing fibers.

Schultz et al. compare different strategies for deciding the appropriate number of fiber compartments, based on the diminishing approximation error [56], thresholding compartment fraction coefficients of a multi-fiber model [58], or by learning the number of fiber compartments using simulated data and support vector regression [54], which represents uncertainty in the form of continuous estimates of fiber number (cf. Fig. 8.5).

Much of the work on determining the number of per-voxel fiber components has been described outside of any particular tractography method, but may nonetheless inform tractographic analysis. Alexander et al. [1] use an F-Test to find an appropriate order of Spherical Harmonic (SH) representation of the ADC profile. Jeurissen et al. [26] decide the number of fibers by counting significant maxima in the fiber orientation distribution after applying the SH deconvolution (constrained by positivity) of Tournier et al. [62]. The SH deconvolution of Tournier et al. [62] in some sense involves model selection, because the deconvolution kernel is modeled by the

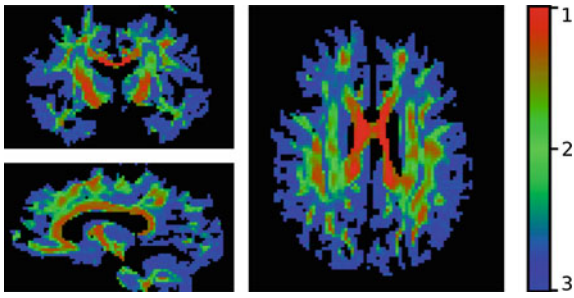

Fig. 8.5 Support vector regression estimates the number of fiber compartments per voxel as a continuous quantity, indicating regions in which a discrete number of fiber compartments can only be determined with considerable uncertainty [54]

SH coefficients of the voxels with the highest FA, presumably representing a single fiber.

Aside from the question of counting fibers, other work has examined more broadly the question of which models of the diffusion weighted signal profile are statistically supported. Bretthorst et al. [8] compute Bayesian evidence (see Sect. 8.4.1) to quantify the fitness of various models of the diffusion weighted signal, producing maps of model complexity in a fixed baboon brain, and of evidence-weighted averages of per-model anisotropy. Freidlin et al. [17] choose between the full diffusion tensor and simpler constrained tensor models according to the Bayesian information criterion (BIC) or sequential application of the F-Test and either the t-Test or another F-Test.

8.3.3 Partial Voluming

Tractography works best in voxels that contain homogeneously oriented tissue. Unfortunately, many regions of the brain exhibit more complex structures, where fibers cross, diverge, or differently oriented fibers pass through the same voxel [1]. This problem is reduced at higher magnetic field strength, which affords increased spatial resolution. However, even at the limit of what is technically possible today [20], a gap of several orders of magnitude remains to the scale of individual axons.

Super-resolution techniques combine multiple images to increase effective resolution. Most such techniques use input images that are slightly shifted with respect to each other and initial success has been reported with transferring this idea to MRI [47]. However, due to the fact that MR images are typically acquired in Fourier space, spatial shifts do not correspond to a change in the physical measurement, so it is unclear by which mechanism repeated measurements should achieve more than an improved signal-to-noise ratio [48, 51]. It is less controversial to compute images that are super-resolved in slice-select direction [18, 52] or to estimate fiber model parameters at increased resolution via smoothness constraints [42].

Track density imaging [10] uses tractography to create super-resolved images from diffusion MRI. After randomly seeding a large number of fibers, the local streamline density is visualized. It is computed by counting the number of lines that run through each element of a voxel grid whose resolution can be much higher than during MR acquisition. Visually, the results resemble those of line integral convolution, which had been applied to dMRI early on [23, 69].

8.4 Perspectives

8.4.1 Evidence for Model Selection

Many of the methods for finding per-voxel fiber count (or more generally the per-voxel signal model) described in Sect. 8.3.2 share two notable properties which may be reconsidered and relaxed in future research. First, they deterministically calculate the single best model, with hard transitions between the regions best explained by one model versus another [1, 17, 26, 50, 56, 58]. Yet we know that partial voluming (Sect. 8.3.3) creates smooth transitions between different neuroanatomic tissue regions. Though computational expensive, Markov Chain Monte Carlo (MCMC) sampling of both model parameter space and the set of models enables averaging information from more than one model [2, 8]. Second, most methods work within a particular hierarchical set of linearly ordered models (SH of different orders [1], ball and multiple sticks [2], sum of higher-order rank-1 terms [58]). One can easily imagine configurations, however, that confound such a linear ordering: an equal mix of two fibers crossing and isotropic diffusion (perhaps due to edema), or a mix of one strong fiber and two weaker equal-strength fibers. Furthermore, there is rarely objective comparison or reconciliation between disjoint sets of models.

An informative perspective on these situations may be gained by directly visualizing, either on data slices or by some form of volume rendering, the fitness of a large palette of possible models. In a Bayesian setting, the model fitness can be quantified by the marginal likelihood of the data $\mathbf{x}$ given the model M_k, or the model *evidence*, computed by integrating over the model parameter space $\boldsymbol{\theta}_k$ [36].

$$\underbrace{P(\mathbf{x}|M_k)}_{\text{evidence}} = \int \underbrace{P(\mathbf{x}|\boldsymbol{\theta}_k, M_k)}_{\text{likelihood}} \underbrace{P(\boldsymbol{\theta}_k|M_k)}_{\text{prior}} d\boldsymbol{\theta}. \tag{8.1}$$

Bretthorst et al. [8] have pioneered the calculation and visualization of model evidence for dMRI, but many possible directions are left unexplored, including the application to counting fibers, and to models that account for intra-voxel fanning or bending [41].

8.4.2 Reproducibility, Seeding, and Preprocessing

The reproducibility of tractography depends on many factors. The manual placement of seed points is an obvious concern. Detailed written instructions improve reproducibility between operators [13], especially across sites [65]. Combining multiple seed regions with logical operators makes the results more reproducible [21, 24] and seeding protocols for up to 11 major fiber bundles have been developed this way [65]. Warping individual brains to a standard template has also been reported to increase

reproducibility [21, 64]. Selecting streamlines from a whole brain tractography via three-dimensional regions of interest [5] or semi-automated clustering [63] is an alternative way to reproducibly extract fiber bundles.

When the same person places the seeds on a repeated scan, the resulting variability is generally higher than when different observers follow a written protocol to place seeds in the same data [13]. Within the same session, measurement noise is the main limiting factor [14]. Between sessions, differences in exact head positioning and other subtle factors increase the variability noticably [64].

Reproducibility suffers even more when repeating the measurement on a different scanner [49]. Even a pair of nominally identical machines has produced a statistically significant bias in Fractional Anisotropy [64]. Improving calibration between sessions or scanners via software-based post-processing appears possible [64], but has not been widely explored so far.

More time consuming measurement protocols generally afford better reproducibility. Even though Heiervang et al. [21] report that the improvement when using 60 rather than 12 gradient directions was not statistically significant, Tensouti et al. [61] report a clear improvement between 6 and 15 directions, which continues—at a reduced rate—when going to 32 directions. Farrel et al. [16] use 30 directions and demonstrate a clear improvement when averaging repeated measurements.

Finally, reproducibility depends on the tractography algorithm [61], its exact implementation [9], as well as the methods used for pre-processing the data [34, 64] and their parameter settings. Given that the reproducibility of tractography will be crucial for its wider acceptance in science and medicine, more work is needed that specifically targets these problems.

8.5 Conclusion

Reproducibility of dMRI tractography is a fundamental problem that limits the acceptance of this technique in clinical practice and neuroscience research. Although some effort has been made to include uncertainty information in the tractography results, several open issues remain that need further investigation.

Probabilistic tractography is established, but visualization research has concentrated on deterministic streamline-based techniques, and few techniques have been developed to visualize the information obtained by probabilistic methods. There are several sources of uncertainty in the tractography visualization pipeline. However, only a few of them have been explored, and if at all studied, they are often considered independently with no connection to each other. Techniques that investigate the impact of parameters on the fiber tracking results and that aim to reduce the impact of user bias through parameter selection have been investigated only recently. Model selection and data preprocessing have hardly been studied with respect to their effects on tractography results.

Techniques that allow the combined analysis of uncertainty from different sources in the same framework, and that facilitate an understanding of their influence on the

final tractography result are still missing. One challenge faced by visualization systems that aim to aid understanding of these uncertainties is to display this additional information efficiently and effectively, without causing visual clutter.

Ultimately, uncertainty visualization should contribute to making fiber tracking a more reliable tool for neuroscience research, and to conveying the information needed for the decision making process in clinical practice.

References

1. Alexander, D.C., Barker, G.J., Arridge, S.R.: Detection and modeling of non-gaussian apparent diffusion coefficient profiles in human brain data. Magn. Reson. Med. **48**, 331–340 (2002)
2. Behrens, T.E.J., Johansen-Berg, H., Jbabdi, S., Rushworth, M.F.S., Woolrich, M.W.: Probabilistic diffusion tractography with multiple fibre orientations: what can we gain? NeuroImage **34**, 144–155 (2007)
3. Behrens, T.E.J., Woolrich, M.W., Jenkinson, M., Johansen-Berg, H., Nunes, R.G., Clare, S., Matthews, P.M., Brady, J.M., Smith, S.M.: Characterization and propagation of uncertainty in diffusion-weighted MR imaging. Magn. Reson. Med. **50**, 1077–1088 (2003)
4. Björnemo, M., Brun, A., Kikinis, R., Westin, C.F.: Regularized stochastic white matter tractography using diffusion tensor MRI. In: Dohi, T., Kikinis, R. (eds.) Proceedings of Medical Image Computing and Computer-Assisted Intervention (MICCAI), Lecture Notes in Computer Science, vol. 2488, pp. 435–442. Springer, Berlin (2002)
5. Blaas, J., Botha, C.P., Peters, B., Vos, F.M., Post, F.H.: Fast and reproducible fiber bundle selection in DTI visualization. In: Silva, C., Gröller, E., Rushmeier, H. (eds) Proceedings of IEEE Visualization, pp. 59–64 (2005)
6. Brecheisen, R., Platel, B., ter Haar Romenij, B.M., Vilanova, A.: Illustrative uncertainty visualization for DTI fiber pathways. In: Poster Proceedings of EuroVis (2011)
7. Brecheisen, R., Vilanova, A., Platel, B., ter Haar Romenij, B.M.: Parameter sensitivity visualization for DTI fiber tracking. IEEE Trans. Vis. Comput. Graph. **15**(6), 1441–1448 (2009)
8. Bretthorst, G.L., Kroenke, C.D., Neil, J.J.: Characterizing water diffusion in fixed baboon brain. In Fischer, R., Preuss, R., von Toussaint, U. (eds.) Bayesian Inference and Maximum Entropy Methods in Science and Engineering, pp. 3–15 (2004)
9. Bürgel, U., Mädler, B., Honey, C.R., Thron, A., Gilsbach, J., Coenen, V.A.: Fiber tracking with distinct software tools results in a clear diversity in anatomical fiber tract portrayal. Cen. Eur. Neurosurg. **70**(1), 27–35 (2009)
10. Calamante, F., Tournier, J.D., Jackson, G.D., Connelly, A.: Track-density imaging (TDI): super-resolution white matter imaging using whole-brain track-density mapping. NeuroImage **53**(4), 1233–1243 (2010)
11. Catani, M., Howard, R.J., Pajevic, S., Jones, D.K.: Virtual in vivo interactive dissection of white matter fasciculi in the human brain. NeuroImage **17**, 77–94 (2002)
12. Chung, S., Ying, L.: Comparison of bootstrap approaches for estimation of uncertainties of DTI parameters. NeuroImage **33**(2), 531–541 (2006)
13. Ciccarelli, O., Parker, G.J.M., Toosy, A.T., Wheeler-Kingshott, C.A.M., Barker, G.J., Boulby, P.A., Miller, D.H., Thompson, A.J.: From diffusion tractography to quantitative white matter tract measures: a reproducibility study. NeuroImage **18**, 348–359 (2003)
14. Ding, Z., Gore, J.C., Anderson, A.W.: Classification and quantification of neuronal fiber pathways using diffusion tensor MRI. Magn. Reson. Med. **49**, 716–721 (2003)
15. Ehricke, H.-H., Klose, U., Grodd, W.: Visualizing MR diffusion tensor fields by dynamic fiber tracking and uncertainty mapping. Comput. Graph. **30**, 255–264 (2006)

16. Farrell, J.A.D., Landman, B.A., Jones, C.K., Smith, S.A., Prince, J.L., van Zijl, P.C.M., Mori, S.: Effects of signal-to-noise ratio on the accuracy and reproducibility of diffusion tensor imaging-derived fractional anisotropy, mean diffusivity, and principal eigenvector measurements at 1.5T. J. Magn. Reson. Imag. **26**, 756–767 (2007)
17. Freidlin, R.Z., Özarslan, E., Komlosh, M.E., Chang, L.-C., Koay, C.G., Jones, D.K., Basser, P.J.: Parsimonious model selection for tissue segmentation and classification applications: a study using simulated and experimental DTI data. IEEE Trans. Med. Imaging **26**(11), 1576–1584 (2007)
18. Greenspan, H., Oz, G., Kiryati, N., Peled, S.: MRI inter-slice reconstruction using super-resolution. Magn. Reson. Imaging **20**, 437–446 (2002)
19. Hagmann, P., Thiran, J.-P., Jonasson, L., Vandergheynst, P., Clarke, S., Maeder, P., Meuli, R.: DTI mapping of human brain connectivity: statistical fibre tracking and virtual dissection. NeuroImage **19**, 545–554 (2003)
20. Heidemann, R.M., Porter, D.A., Anwander, A., Feiweier, T., Calamante, F., Tournier, J.-S., Lohmann, G., Meyer, H., Knösche, T.R., Turner, R.: Whole-brain, multi-shot, diffusion-weighted imaging in humans at 7T with 1 mm isotropic resolution. In Proceedings of International Society of Magnetic Resonance in Medicine (ISMRM), p. 417 (2011)
21. Heiervang, E., Behrens, T.E.J., Mackay, C.E., Robson, M.D., Johansen-Berg, H.: Between session reproducibility and between subject variability of diffusion MRI and tractography measures. NeuroImage **33**, 867–877 (2006)
22. Hoeting, J.A., Madigan, D., Raftery, A.E., Volinsky, C.T.: Bayesian model averaging: a tutorial. Stat. Sci. **14**(4), 382–417 (1999)
23. Hsu, E.: Generalized line integral convolution rendering of diffusion tensor fields. In Proceedings of International Society of Magnetic Resonance in Medicine (ISMRM), p. 790 (2001)
24. Hao, H., Zhang, J., van Zijl, P.C.m., Mori, S.: Analysis of noise effects on DTI-based tractography using the brute-force and multi-ROI approach. Magn. Reson. Med. **52**, 559–565 (2004)
25. Hubbard, P.L., Parker, G.J.M.: Validation of tractography. In: Johansen-Berg, H., Behrens, T.E.J. (eds.) Diffusion MRI: From Quantitative Measurement to in-Vivo Neuroanatomy, pp. 353–375. Academic Press, Massachusetts (2009)
26. Jeurissen, B., Leemans, A., Tournier, J-D. Jones, D.K., Sijbers, J.: Estimating the number of fiber orientations in diffusion MRI voxels: a spherical deconvolution study. In Proceedings of International Society of Magnetic Resonance in Medicine (ISMRM) (2010)
27. Jeurissen, B., Leemans, A., Jones, D.K., Tournier, J.D., Sijbers, J.: Probabilistic fiber tracking using the residual bootstrap with constrained spherical deconvolution. Hum. Brain Mapp. **32**, 461–479 (2011)
28. Jiao, F., Phillips, J.M., Gur, Y., Johnson, C.R.: Uncertainty visualization in HARDI based on ensembles of ODFs. In: Hauser, H., Kobourov, S.G., Qu, H. (eds.) Proceedings of IEEE Pacific Visualization Symposium, pp. 193–200 (2012)
29. Jiao, F., Phillips, J.M., Stinstra, J., Krüger, J., Varma, R., Hsu, E., Korenberg, J., Johnson, C.R.: Metrics for uncertainty analysis and visualization of diffusion tensor images. In: Liao, H., Eddie Edwards, P.J., Pan, X., Fan, Y., Yang, G.-Z. (eds.) Proceedings of Medical Imaging and Augmented Reality. Lecture Notes in Computer Science, vol. 6326, pp. 179–190 (2010)
30. Jones, D.K., Travis, A.R., Eden, G., Pierpaoli, C., Basser, P.J.: Pasta: pointwise assessment of streamline tractography attributes. Magn. Reson. Med. **53**(6), 1462–1467 (2005)
31. Jones, D.K.: Determining and visualizing uncertainty in estimates of fiber orientation from diffusion tensor MRI. Magn. Reson. Med. **49**, 7–12 (2003)
32. Jones, D.K.: Tractography gone wild: probabilistic fibre tracking using the wild bootstrap with diffusion tensor MRI. IEEE Trans. Med. Imaging **27**(9), 1268–1274 (2008)
33. Jones, D.K.: Challenges and limitations of quantifying brain connectivity in vivo with diffusion MRI. Future Med. **2**(3), 341–355 (2010)
34. Jones, D.K., Cercignani, M.: Twenty-five pitfalls in the analysis of diffusion MRI data. NMR Biomed. **23**, 803–820 (2010)
35. Jones, D.K., Pierpaoli, C.: Confidence mapping in diffusion tensor magnetic resonance imaging tractography using a bootstrap approach. Magn. Reson. Med. **53**, 1143–1149 (2005)

36. Kass, R.E., Raftery, A.E.: Bayes factors. J. Am. Stat. Assoc. **90**(430), 773–795 (1995)
37. Kinoshita, M., Yamada, K., Hashimoto, N., Kato, A., Izumoto, S., Baba, T., Maruno, M., Nishimura, T., Yoshimine, T.: Fiber-tracking does not accurately estimate size of fiber bundle in pathological condition: initial neurosurgical experience using neuronavigation and subcortical white matter stimulation. NeuroImage **25**(2), 424–429 (2005)
38. Koch, M.A., Norris, D.G., Hund-Georgiadis, M.: An investigation of functional and anatomical connectivity using magnetic resonance imaging. NeuroImage **16**, 241–250 (2002)
39. Lazar, M., Alexander, A.L.: Bootstrap white matter tractography (BOOT-TRAC). NeuroImage **24**(2), 524–532 (2005)
40. McGraw, T., NadarM.S.: Stochastic DT-MRI connectivity mapping on the GPU. IEEE Trans. Visual. Comput. Graph. **13**(6), 1504–1511 (2007)
41. Nedjati-Gilani, S., Alexander, D.C.: Fanning and bending sub-voxel structures in diffusion MRI. In Proceedings International Society of Magnetic Resonance in Medicine (ISMRM), p. 1402 (2009)
42. Nedjati-Gilani, S., Alexander, D.C., Parker, G.J.M.: Regularized super-resolution for diffusion MRI. In Proceedings of IEEE International Symposium on Biomedical Imaging (ISBI), pp. 875–878 (2008)
43. Pajevic, S., Basser, P.J.: Parametric and non-parametric statistical analysis of DT-MRI data. J. Magn. Reson. **161**(1), 1–14 (2003)
44. Parker, G.J.M., Alexander, D.C.: Probabilistic monte carlo based mapping of cerebral connections utilising whole-brain crossing fibre information. In: Taylor, C.J., Noble, J.A. (eds.) Information Processing in Medical Imaging. Lecture Notes in Computer Science, vol. 2732, pp. 684–695. Springer, Berlin (2003)
45. Parker, G.J.M., Haroon, H.A., Wheeler-Kingshott, C.A.M.: A framework for a streamline-based probabilistic index of connectivity (pico) using a structural interpretation of MRI diffusion measurements. J. Magn. Reson. Imaging **18**, 242–254 (2003)
46. Peled, S., Friman, O., Jolesz, F., Westin, C.-F.: Geometrically constrained two-tensor model for crossing tracts in DWI. Magn. Reson. Imaging **24**(9), 1263–1270 (2006)
47. Peled, S., Yeshurun, Y.: Superresolution in MRI: application to human white matter fiber tract visualization by diffusion tensor imaging. Magn. Reson. Med. **45**, 29–35 (2001)
48. Peled, S., Yeshurun, Y.: Superresolution in MRI—perhaps sometimes. Magn. Reson. Med. **48**, 409 (2002)
49. Pfefferbaum, A., Adalsteinsson, E., Sullivan, E.V.: Replication of diffusion tensor imaging measurements of fractional anisotropy and trace in brain. J. Magn. Reson. Imaging **18**, 427–433 (2003)
50. Qazi, A.A., Radmanesh, A., O'Donnell, L., Kindlmann, G., Peled, S., Whalen, S., Westin, C.-F., Golby, A.J.: Resolving crossings in the corticospinal tract by two-tensor streamline tractography: method and clinical assessment using fMRI. NeuroImage, **47**(Supplement 2), T98–T106 (2009, in press)
51. Scheffler, K.: Superresolution in MRI? Magn. Reson. Med. **48**, 408 (2002)
52. Scherrer, B., Gholipour, A., Warfield, S.K.: Super-resolution in diffusion-weighted imaging. In: Fichtinger, G., Martel, A., Peters, T. (eds.) Proceedings of Medical Image Computing and Computer-Assisted Intervention (MICCAI). Lecture Notes in Computer Science, vol. 6892, pp. 124–132. Springer, Berlin (2011)
53. Schultz. T.: Feature extraction for visual analysis of DW-MRI data. Ph.D. thesis, Universität des Saarlandes (2009)
54. Schultz, T: Learning a reliable estimate of the number of fiber directions in diffusion MRI. In: Ayache, N. et al. (eds.) Proceedings of Medical Image Computing and Computer-Assisted Intervention (MICCAI), pp. 493–500 (2012) (Part III volume 7512 of LNCS)
55. Schultz, T., Schlaffke, L., Schölkopf, B., Schmidt-Wilcke, T.: HiFiVE: a Hilbert space embedding of fiber variability estimates for uncertainty modeling and visualization. Comput. Graph. Forum **32**(3), 121–130 (2013)
56. Schultz, T., Seidel, H.P.: Estimating crossing fibers: a tensor decomposition approach. IEEE Trans. Visual. Comput. Graph. **14**(6):1635–1642 (2008)

57. Schultz, T., Theisel, H., Seidel, H.P.: Topological visualization of brain diffusion MRI data. IEEE Trans. Visual. Comput. Graph. **13**(6), 1496–1503 (2007)
58. Schultz, T., Westin, C.F., Kindlmann, G.: Multi-diffusion-tensor fitting via spherical deconvolution: a unifying framework. In Jiang, T. et al. (eds.) Proceedings of Medical Image Computing and Computer-Assisted Intervention (MICCAI), pp. 673–680. Springer, Berlin (2010) (vol. 6361 of Lecture Notes in Computer Science)
59. A.J. Sherbondy, R.F. Dougherty, M. Ben-Shachar, S. Napel, and B. Wandell. Contrack: Finding the most likely pathways between brain regions using diffusion tractography. Journal of Vision, 8:1, 2008.
60. Sotiropoulos, S.N., Jbabdi, S., Xu, J., Andersson, J.L., Moeller, S., Auerbach, E.J., Glasser, M.F., Hernandez, M., Sapiro, M., Jenkinson, M., Feinberg, D.A., Yacoub, E., Lenglet, C., Van Essen, D.C., Ugurbil, K., Behrens, T.E.J.: Advances in diffusion MRI acquisition and processing in the human connectome project. NeuroImage. doi:10.1016/j.neuroimage.2013.05.057 (2013)
61. Tensaouti, F., Lahlou, I., Clarisse, P., Lotterie, J.A., Berry, I.: Quantitative and reproducibility study of four tractography alorithms used in clinical routine. Journal of Magnetic Resonance Imaging **34**, 165–172 (2011)
62. Tournier, J.D., Calamante, F., Connelly, A.: Non-negativity constrained super-resolved spherical deconvolution: robust determination of the fibre orientation distribution in diffusion MRI. NeuroImage **35**, 1459–1472 (2007)
63. Voineskos, A.N., O'Donnell, L.J., Lobaugh, N.J., Markant, D., Ameis, S.H., Niethammer, M., Mulsant, B.H., Pollock, B.G., Kennedy, J.L., Westin, C.-F., Shenton, M.E.: Quantitative examination of a novel clustering method using magnetic resonance diffusion tensor tractography. NeuroImage **45**(2), 370–376 (2009)
64. Vollmar, C., O'Muircheartaigh, J., Barker, G.J., Symms, M.R., Thompson, P., Kumari, V., Duncan, J.S., Richardson, M.P., Koepp, M.J.: Identical, but not the same: intra-site and inter-site reproducibility of fractional anisotropy measures on two 3.0 T scanners. NeuroImage **51**(4), 1384–1394 (2010)
65. Wakana, S., Caprihan, A., Panzenboeck, M.M., Fallon, J.H., Perry, M., Gollub, R.L., Hua, K., Zhang, J., Jiang, H., Dubey, P., Blitz, A., van Zijl, P., Mori, S.: Reproducibility of quantitative tractography methods applied to cerebral white matter. NeuroImage **36**, 630–644 (2007)
66. Westin, C.F., Peled, S., Gubjartsson, H., Kikinis, R., Jolesz, F.A.: Geometrical diffusion measures for MRI from tensor basis analysis. In Proceedings of International Society of Magnetic Resonance in Medicine (ISMRM) (1997)
67. Whitcher, B., Tuch, D.S., Wisco, J.J., Gregory Sorenson, A., Wang, L.: Using the wild bootstrap to quantify uncertainty in DTI. Human Brain Map. **29**(3), 346–362 (2008)
68. Wu, J.S., Mao, Y., Zhou, L.F., Tang, W.J., Hu, J., Song, Y.Y., Hong, X.N., Du, G.H.: Clinical evaluation and follow-up outcome of diffusion tensor imaging-based functional neuronavigation: a prospective, controlled study in patients with gliomas involving pyramidal tracts. Neurosurgery **61**(5), 935–949 (2007)
69. Zheng, X., Pang, A.: HyperLIC. In Proceedings of IEEE Visualization, pp. 249–256 (2003)